

Phosphoniumyl cationic porphyrins

Self-aggregation origin from π - π and cation- π interactions

Ren-Hua Jin,* Shinya Aoki and Kensuke Shima

Department of Materials Science, Faculty of Engineering, Miyazaki University, Miyazaki 889-21, Japan

The electro spectroscopic properties of four cationic porphyrins possessing phosphonium residues in the periphery of the porphyrin plane are investigated in aqueous and organic solvent phases. The electronic spectra of the phosphoniumyl porphyrins in pure water and in the presence of inorganic and organic electrolytes are compared, and it is proposed that self-aggregation of the phosphoniumyl porphyrins arises from π - π interaction forming H-aggregates and that this geometry can be transformed into J-aggregates by cation- π interaction between the porphyrin plane and the peripheral phosphonium cations on addition of NaCl. ^1H NMR spectra provide evidence that the highly polarizable phosphonium cation interacts strongly with the highly polarizable porphyrin π -surface.

Introduction

Water soluble cationic porphyrins are currently of interest because of their possible wide applications, such as in supramolecular architecture, in photochemical cleavage of DNA, in water splitting reactions and as mimics of energy transfer systems.¹ Most attention has focused on the tetrakis(methylpyridiniumyl)porphyrins (TPyPs), and the fundamental research about TPyPs in the area of solution chemistry has concluded some inconsistent results from various independent groups.² Compared with organic solvent soluble porphyrin systems, where a large number of well-defined porphyrins have significant roles in chemistry,³ water soluble cationic porphyrins have not been systematically documented, probably because not much effort has been made towards their synthesis. Many of the reports concerning water soluble cationic porphyrins have argued that the peripheral structures of the porphyrin plane play an important role in their incorporation of guest molecules and also their self-assembly properties.⁴ In the cationic porphyrin systems, our interest is mainly aimed at the following ideas. First, the macrocyclic π -plane of the cationic porphyrin not only has a strong hydrophobic feature but is also highly polarizable. Thus, porphyrins dissolved in water do not allow many water molecules to lie over the π -plane. Second, the π -surface of the porphyrin is electronically negative due to the quadrupole moment of the quadrupole moment of the π -plane and this makes it possible to promote the cation- π interaction between the face of the porphyrin and the cation. In view of the recent progress in molecular recognition and biomimetic systems, one of the most interesting events is the cation- π interaction;⁵ this interaction plays an extremely important role in water soluble molecular systems, such as in the structure and function of proteins, and in ion channels and in molecular recognition hosts.

With regard to their structural character, the cationic porphyrins are a family bearing onium units, such as ammonium (or pyridinium), phosphonium and sulfonium. However, the cationic porphyrins researched so far are almost limited to the nitrogen cationic centre, including ammonium and pyridinium. Our interest is the introduction of nitrogen, phosphorus and sulfur atoms into the periphery of the porphyrin.

For this purpose, a derivative of tetra(phenyl)porphyrin bearing active chloromethyl groups in the *para*-position of the *meso*-phenyl ring was synthesized,⁶ so that the chloromethyl group could be reacted with amines, pyridines, phosphines and sulfides as well as many nucleophiles in order to yield the corresponding cationic porphyrins or other derivatives. In this paper, we report the solution chemistry of a new cationic porphyrin family containing phosphonium units in both aqueous and organic media.

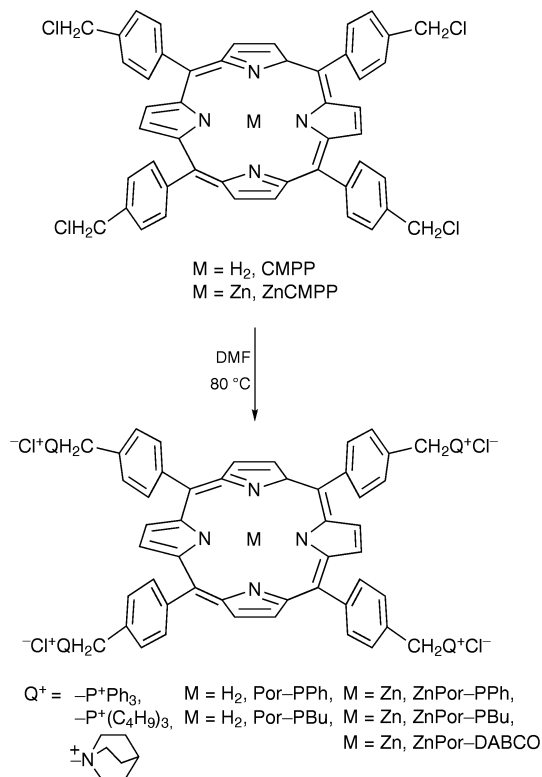
Results

Synthesis

As shown in Scheme 1, the cationic porphyrins Por-PPh, Por-PBu, ZnPor-PPh, ZnPor-PBu, ZnPor-DABCO (DABCO = diazabicyclo[2.2.2]octane) were conveniently obtained from the reaction of tetrakis(*p*-chloromethylphenyl)porphyrin (CMPP) or ZnCMPP with the corresponding phosphine or amine (DABCO). In particular, the reaction between ZnCMPP and DABCO was very facile and yielded quantitatively the corresponding cationic porphyrin (possessing DABCO residues) within 2 h. This result is significantly different to those for trialkylamines, such as $\text{N}(\text{C}_2\text{H}_5)_3$ and $\text{N}(\text{C}_4\text{H}_9)_3$, which required long reaction times⁶ (data not listed). All the cationic porphyrins gave satisfactory structures as determined by ^1H NMR.

Soret bands and the environment

The phosphoniumyl porphyrins, Por-PPh, Por-PBu, ZnPor-PPh, ZnPor-PBu, have four positive charges in the periphery of the π -plane of the porphyrins. The cationic sites are separated within the TPP framework by methylene bridges. Thus, these tetra-cationic porphyrins are distinguishable from previous cationic porphyrins, such as TPyPs and tetra(trimethylammoniumylphenyl)porphyrin (whose cationic centres can influence the electronic density of the *meso*-phenyl or pyridyl rings by an inductive effect). For TPyPs, the positive charge on the pyridinium nitrogen atoms may be delocalized over the porphyrin plane through resonance structures.^{2f} Because the above porphyrins prevent the delocalization of the positive charges of the cations, there will be less of a bonding effect from the cations on the electronic properties of the porphyrin



Scheme 1

plane. In other words, the electronic properties of the flat π -surfaces of the non-cationic CMPP and the cationic porphyrins must be identical. With this in mind, we made a detailed investigation of the Soret bands of these porphyrins in aqueous and organic solutions.

Solvent and wavelength. Table 1 shows the wavelength of the Soret bands for the cationic and neutral porphyrins in several organic solvents and/or in water. The wavelength of CMPP (which is insoluble in water) shifted in the range 413.5–419.2 nm with different solvents; the wavelength shift is related to the solvent polarizability (discussed below). The other cationic porphyrins also displayed similar responses, although the cationic substituents are different each other. Apparently, the Soret bands for the cationic porphyrins appeared at longer wavelengths in DMSO but were blue-shifted in MeOH. It should be noted that the cationic porphyrins are freely soluble in both DMSO and MeOH, but the behavior of the porphyrins are opposite in these two solvents.

Effect of concentration. By using water and methanol as solvents, we determined the relationship between concentration and the Soret band. The details are summarized in Table 2, where wavelength (λ_{\max}), absorbance (A) at λ_{\max} and band-

Table 1 Soret bands of porphyrins in various solvents^a

solvent	$\alpha/\text{\AA}^3$	λ_{\max}/nm			
		TTP ^b	CMPP	Por-PPh	Por-PBu
H ₂ O	1.47			415.7	413.6
MeOH	3.28	413.4	413.5	415.2	414.8
MeCN	4.86	414.3	414.0	416.0	415.3
acetone	6.33	414.7	414.7	416.6	416.1
DMF	7.31	417.9	418.1	419.2	418.8
CHCl ₃	8.34	419.2	419.2	420.6	420.1
DMSO	8.87	419.2	419.2	420.0	420.0

^a Concentration of the porphyrins was ca. 5 μM . ^b TTP = 5, 10, 15, 20-tetra-*p*-tolylporphyrin.

width at half-height peak ($W_{1/2}$) are listed. The wavelength for Por-PPh remained constant at 416 nm without any concentration dependence, but the Soret band for Por-PBu was shifted to 415 nm from 422 nm as the concentration was increased from 0.1 to 10 μM . It is very interesting that when the concentration of Por-PBu was adjusted to 2.0 μM , two peaks from Soret bands at 420.0 and 415.0 nm with absorbances of 0.588 and 0.576 (see Fig. 1) appeared. At this concentration $W_{1/2}$ also increased significantly. Above this concentration, the Soret bands became one peak at a blue-shifted wavelength of 414.8 nm. By using water as solvent instead of methanol in this experiment, we observed a different tendency. In water, the band-width was significantly increased as the concentration was increased although the wavelength for the Soret band of Por-PPh did not change. For Por-PBu in water the Soret band appeared at a relatively short wavelength (414 nm) even over a wide concentration range, and the band width only increased at higher concentration (10 μM). For both ZnPor-PPh and ZnPor-PBu in aqueous medium, the concentration of porphyrins significantly influenced the Soret band peak (see Table 2). λ_{\max} appeared above 430 nm at extremely dilute concentrations (*e.g.* 0.1–0.5 μM); over this concentration the Soret band was greatly blue-shifted (by 8–10 nm). However, with MeOH the Soret band appeared at 422–424 nm with both high and lower concentrations of zinc phosphoniumyl porphyrins.

Soret band and NaCl effect. Many reports about water soluble cationic or anionic porphyrins demonstrate that aggregation of porphyrins takes place as electrolytes are added. In general, addition of electrolytes, such as KNO₃, NaCl and KCl, makes the Soret band red-shift.^{2b,7} Compared with the Soret bands for the aggregates caused by the concentration of porphyrins, the aggregates induced by addition of electrolytes have significantly different Soret bands.

As summarized in Table 3, the phosphoniumyl porphyrins exhibited a unique change in response to the concentration of NaCl. Por-PPh (5 μM) in water showed a very broad Soret band at 415.8 nm. Addition of 0.1 M NaCl to an aqueous solution of Por-PPh caused a red-shift (427.5 nm) of the Soret band and a lower absorbance. When the concentration of NaCl increased to 0.3 M the Soret band split into three peaks, appearing at 407, 427 and 441 nm (see Table 3 and Fig. 2).

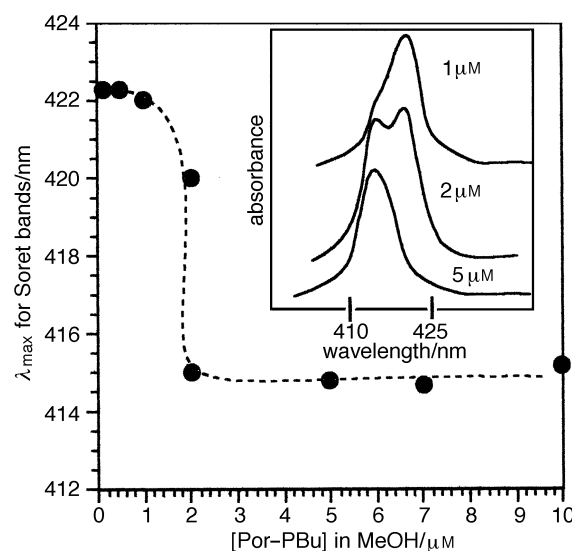


Fig. 1 Plot of λ_{\max} for the Soret band versus the concentrations of Por-PBu in methanol. Inset: profiles of UV-VIS spectra at different concentrations of Por-PBu.

Table 2 Soret bands of tetracationic porphyrins in methanol and water

	conc./ μM	MeOH			H ₂ O		
		$\lambda_{\text{max}}/\text{nm}$	$W_{1/2}/\text{nm}$	A	$\lambda_{\text{max}}/\text{nm}$	$W_{1/2}/\text{nm}$	A
Por-PPh	0.1	415.9	12.5	0.026			
	0.5	415.4	12.6	0.151	415.6	16.3	0.071
	1.0	415.6	12.6	0.401	416.0	21.3	0.143
	2.0	415.2	12.6	0.789	416.0	24.5	0.337
	5.0	415.2	15.0	1.922	416.4	27.0	1.087
	7.0	415.5	16.3	2.254	416.4	28.8	1.46
	10	416.0	18.8	2.372	416.4	29.5	1.83
	Por-PBu	0.1	422.3	10	0.027		
0.5		422.3	12	0.182	413.5	12.5	0.038
1.0		422.0	13.8	0.376	414.0	12.5	0.245
2.0		420.0/415.0	17.5	0.588/0.576	414.0	12.5	0.491
5.0		414.8	17.5	1.523	413.6	13.5	1.528
7.0		414.7	17.5	2.013	413.5	14.8	1.896
10		415.2	18.8	2.292	413.9	17.5	2.237
ZnPor-PPh		0.1	423.9	10	0.048	432.9	25
	0.5	424.0	9.5	0.292	431.8	25	0.070
	1.0	424.0	9.8	0.596	426.0	25	0.138
	2.0	424.0	9.5	1.195	424.0	22	0.410
	5.0	424.0	11.8	2.138	423.1	22	1.321
	7.0	423.4	14.3	2.210	423.5	23	1.793
	10	423.9	17	2.243	424.1	25	2.172
	ZnPor-PBu	0.1	422.5	9.0	0.022	430.7	27.7
0.5		423.0	10	0.269	431.6	27.7	0.045
1.0		422.9	10	0.550	422.0	13.8	0.206
2.0		422.7	9.3	1.105	422.0	12.3	0.547
5.0		422.5	11.8	2.067	421.6	14.3	1.614
7.0		421.5	13.8	2.150	421.6	15.8	2.075
10		419.7	16.8	2.195	420.1	21.8	2.273

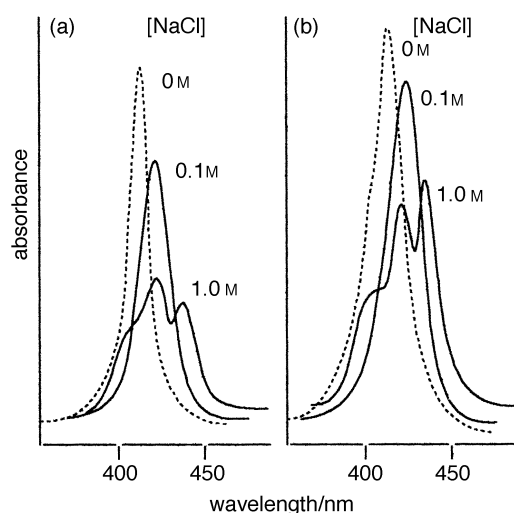


Fig. 2 Absorption spectra of (a) Por-PBu and (b) Por-PPh at different concentrations of NaCl. Porphyrin concentration = 5 μM . Split band: (a) 409.3, 423.0 and 438.9 nm (1.0 M NaCl); (b) 407.4, 426.9 and 441.1 nm (0.3 M NaCl).

Further increase in the concentration of NaCl, to 1.0 M, did not change this pattern. At a concentration of NaCl of 2.0 M, the bands formed one band at 427 nm. A similar result was also observed for Por-PBu. The Soret band of Por-PBu was abruptly red-shifted from 413.8 nm (in the absence of NaCl) to 425.7 nm (in the presence of NaCl) and the absorbance was markedly decreased. The Soret band at 425 nm was split into three peaks when the concentration of NaCl was increased to 1.0 M. A longer wavelength peak appeared at 439 nm and a shorter wavelength peak was seen at 409 nm (Fig. 2). However, for ammonium cationic porphyrins with triethyl- or tributyl-ammonium residues splitting of the Soret band and large red-shifts were not observed (data not shown) even when NaCl was added over a wide concentration range. The addition of NaCl to the solutions of zinc phosphonium porphyrins, ZnPor-PPh and ZnPor-PBu, gave different results. The Soret band for ZnPor-PPh was significantly red-shifted to 448 nm, but the half-width remained at 33 nm. For ZnPor-PBu the Soret band red-shifted with a dramatic decrease in absorption, the half-width also increased significantly as the concentration of NaCl increased; the largest wavelength shift was 9 nm (Table 4).

Table 3 Effect of concentration of NaCl on the Soret band of phosphonium porphyrins^a

[NaCl]/M	Por-PPh		Por-PBu	
	$A(\lambda_{\text{max}}/\text{nm})$	$A(\lambda_{\text{max}}/\text{nm})$	$A(\lambda_{\text{max}}/\text{nm})$	$A(\lambda_{\text{max}}/\text{nm})$
0.0	1.116(415.8)		1.488(413.8)	
0.1	0.838(427.5)		0.978(425.7)	
0.3	0.329(407.4)	0.553(426.9)	0.937(425.1)	
0.5	0.364(407.9)	0.598(426.9)	0.875(425.1)	
0.7	0.359(407.3)	0.593(425.9)	0.690(425.0)	
1.0	0.334(407.4)	0.530(425.9)	0.546(424.2)	0.420(439.2)
2.0		0.526(425.9)	0.459(439.1)	0.481(438.9)
			0.424(409.3)	

^a Concentration of porphyrins in H₂ is 5 μM .

Table 4 Effect of concentration of NaCl on the Soret band of zinc phosphoniumyl porphyrins^a

[NaCl]/M	ZnPor-PPh			ZnPor-PBu	
	$A(\lambda_{\max}/\text{nm})^b$	$W_{1/2}/\text{nm}$		$A(\lambda_{\max}/\text{nm})^c$	$W_{1/2}/\text{nm}$
0.0	1.190(424.4)		23.0	1.614(422.0)	12.5
0.1	0.980(431.8)	1.023(435.9)	24.5	1.168(424.2)	1.161(427.6)
0.3		0.726(440.0)	35.8	1.100(425.9)	1.100(428.0)
0.5			33.0	1.020(425.4)	1.008(428.4)
0.7		0.831(448.4)	33.0	0.819(424.9)	0.770(430.9)
1.0		0.763(447.6)	33.8	0.341(426.9)	—
2.0		0.781(448.4)	34.3	0.45(broad peak 430–450)	49.5

^a Concentration of porphyrins in H₂O is 5 μM . ^b Peak with shoulder at longer wavelength appeared. ^c Peak with shoulder at shorter wavelength appeared when NaCl was added.

The results above indicate that the aggregation of cationic porphyrins is strongly influenced by the addition of electrolyte; the aggregation behaviors differed depending on the cationic center, the substituents and the central metal.

Effect of anionic aromatic electrolyte. Anionic or cationic aromatic compounds are usually used with cationic and anionic porphyrin systems in order to establish interaction models for porphyrins with substrates.^{7a,8} Here, anthraquinone-2,6-disulfonic acid disodium salt (DSAQ) was selected as the anionic aromatic electrolyte, and its effects on the Soret band of the cationic porphyrins were investigated.

Compared with the effects of NaCl on the Soret bands, the influence of DSAQ started at very low concentrations, *e.g.*, micromolar ranges. Setting the porphyrin concentration at 5 μM , we varied the concentrations of DSAQ from 5 to 100 μM . For Por-PPh, the addition of an equimolar amount of DSAQ made the Soret band red-shift from 416 nm (without DSAQ) to 426 nm and resulted in a decrease in absorbance (see Table 5). As the DSAQ concentration was increased to twice equimolar, the Soret band was split into three peaks (similar to the case when adding NaCl). When the molar ratio of DSAQ to porphyrin was >14, the three bands recombined into one band, which is also seen with NaCl. Hence, it can be said that aggregates having the same geometry resulted from both inorganic and aromatic sodium salts. The Soret band for ZnPor-PPh was only red-shifted to 434 nm, even when the concentration of DSAQ was increased significantly. On the other hand, the free-base form of the butyl-substituted phosphoniumyl porphyrin, Por-PBu, did not show the Soret band splitting under the same experimental conditions (see Table 5), although it did split in the presence of NaCl. As the ratio of porphyrin to DSAQ was increased, the Soret band for Por-PBu gradually red-shifted from 413 nm to 423 nm, the band-width increased dramatically accompanied by a reduction in absorbance.

Discussion

All the results described above are very interesting with regard to the investigation of the structure-medium-aggregate rela-

tion. Hence, we believe that interpretation of these results will be very important in establishing the interaction mechanism that relates to the formation of monomeric, dimeric, and polymeric cationic porphyrins. As with many other spectroscopic techniques,⁹ such as fluorescence spectrometry, NMR, EPR, Raman spectrometry and dynamic photolysis, UV-VIS spectroscopy is a very prominent and simple tool to aid research into the ground-state chemistry of porphyrins and information obtained from UV-VIS spectroscopy is also valid for use in gaining an understanding of the geometry of the aggregates.¹⁰ We found that the Soret bands of the cationic porphyrins used here were very sensitive to several factors, such as the solvent, the concentration of the porphyrins and the addition of electrolytes, whereas the Q-bands are far less affected by these factors.

The effect of concentration on the Soret band showed that for a defined concentration of Por-PBu two Soret bands appeared at 420 and 415 nm; below this defined concentration one Soret band was observable at longer wavelength and above this concentration a single Soret band appeared at shorter wavelength. Such a 'critical concentration' (CC) was also observable for the zinc forms of the phosphoniumyl cationic porphyrins. This phenomenon strongly suggests that these porphyrins exist mainly as monomers below the CC but as dimers over the CC. The dimers should contribute to the formation of face-to-face geometry because of the blue-shift of the Soret band.^{4a,10d,11} In the relations between the Soret band absorbance and the concentrations in both water and methanol, we did not find that Beer's law was obeyed for the cationic porphyrins. In particular, Por-PPh exhibited an extremely broad band with a shoulder (at shorter wavelength) in water. However, in DMSO solution, it was found that a plot of the absorbance of the Soret band (at 420 nm) *versus* the concentration of Por-PPh (to 5 μM) gave a linear relation, with a constant band-width (see Table 6) of 15 nm. The effect of solvent is also evident from the ¹H NMR spectra for Por-PPh (Fig. 3). The β -protons give a sharp single peak in [²H₆]DMSO that broadens in [²H₄]methanol. In D₂O, the total signal becomes complex with other new peaks appearing. From these results, it could be concluded that Por-PPh is favored to exist as a monomer in DMSO. We can see from

Table 5 Effect of concentration of DSAQ on the Soret band of phosphoniumyl porphyrins^a

[DSAQ]/[Por]	Por-PPh			Por-PBu		ZnPor-PPh	
	$A(\lambda_{\max}/\text{nm})$	$W_{1/2}/\text{nm}$		$A(\lambda_{\max}/\text{nm})$	$W_{1/2}/\text{nm}$	$A(\lambda_{\max}/\text{nm})$	$W_{1/2}/\text{nm}$
0	1.116(415.8)			1.488(413.8)	13.3	1.280(423.1)	20.8
1.0	0.613(426.0)			0.725(419.2)	27.5	0.982(427.9)	27.0
1.4	0.614(427.2)			0.726(420.4)	31.3	0.836(431.0)	27.0
2.0	0.146(409.0)	0.348(429.2)	0.304(440.3)	0.703(420.2)	30.5	0.585(432.7)	26.8
6.0	0.131(409.0)	0.248(429.0)	0.242(441.5)	0.616(421.5)	35.0	0.699(433.8)	28.8
10	0.115(409.0)	0.214(429.9)	0.204(441.1)	0.476(422.0)	39.5	0.645(434.7)	30.0
14	0.109(409.0)	0.198(429.9)	0.187(441.6)	0.459(421.6)	40.0	0.592(436.0)	30.0
20		0.483(429.2)		0.476(423.1)	40.5	0.614(434.4)	30.0

^a Concentration of porphyrins in H₂O is 5 μM .

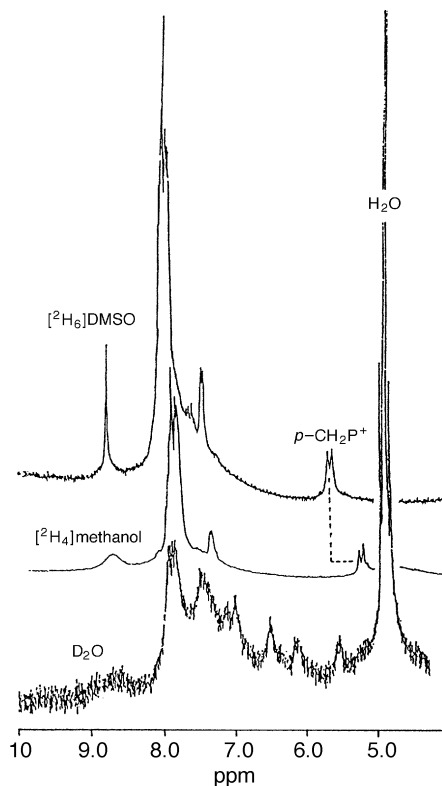


Fig. 3 ^1H NMR profiles of Por-PPh in different deuterated solvents. For D_2O , 10% v/v deuterated methanol was included to dissolve the Por-PPh completely.

Table 1 that λ_{max} evidently blue-shifts with decreasing solvent polarizability, this is because of the high polarizability (60.97 \AA^3 for the π -plane) of porphyrin,^{12,13} *i.e.*, a highly polarizable solvent interacts effectively with the highly polarizable π -plane of the porphyrin. Therefore, the π -plane of the porphyrin can be sufficiently isolated in the solvent 'cluster', and the solvated π -face hardly aggregates together. Water and methanol have high cohesive interactions even though their molecular polarizabilities are very low. This feature often promotes the hydrophobic and/or van der Waals interactions between the apolar solutes dissolved in water and leads to aggregation.¹⁴ This is also possible with the cationic porphyrin used in this work; little of the water lies on the highly polarizable and largely hydrophobic¹⁵ porphyrin plane. Hence, we think that an interaction between the π -surface and the low polarizability solvent is unfavorable. It is probable that for this reason the porphyrin stacks in water and in MeOH give face-to-face aggregates. For Por-PPh in aqueous solution, the extremely wide band-width probably means that there are some other species present, including dimers and oligomers (the ^1H NMR profile in D_2O also supports this possibility). However, in methanol, the dimer must be the major aggregating species. Other cationic porphyrins, *e.g.* Por-PBu, and zinc forms also exist as dimers in water. In DMSO the cationic porphyrins and

neutral CMPP exist as monomers because DMSO has a relatively high polarizability. DMSO inhibits the interaction between the π -surfaces of the porphyrins, even for a porphyrin dimer linked covalently face-to-face.¹⁶ The cationic porphyrins are less soluble in chloroform. The Soret band appeared at 420 nm indicating that the cationic porphyrins exist as monomers due to the high polarizability of chloroform. DMF also inhibits self-aggregation of the porphyrins. Previous reports about anionic and/or cationic porphyrins describe self-dimerization with a face-to-face model in which the peripheral octa-ionic charges take a cross-arranged geometry^{8b} to overcome charge repulsion. The dimeric form has octacationic charges but the area of its hydrophobic surface is the same as that of a monomer, so that the hydrophilicity of the dimer can become larger than that of monomers.

As described above (Table 5 and Fig. 2), addition of electrolytes (inorganic and aromatic) to the dimeric (or polymeric) porphyrins in aqueous solution induced a red-shift of the Soret bands. However, the extent and pattern of the red-shift are different for each cationic porphyrin. Por-PPh ($5 \mu\text{M}$) in water shows a Soret band at 416 nm, which red-shifted by 10 nm at a defined concentration of NaCl or DSAQ. A further increase in the concentration of the electrolytes induced a split of the band at 427 nm and two extra peaks appeared (one at a higher and one at a lower wavelength). This indicates that the species absorbing at 427 nm were transformed into different species. Two problems now attract our attention: (i) why do the inorganic sodium salt and the aromatic sodium salt lead to the same spectra and (ii) what species are formed after addition of the electrolytes. Inorganic electrolytes that induce aggregation of ionic porphyrins have been reported previously.^{2b,7} It is generally believed that neutralization of the positively or negatively charged porphyrins by the inorganic electrolytes reduces the electrostatic repulsion between the ionic charges on the periphery of the porphyrins so that aggregation takes place more easily. For Por-PPh, the split of the Soret band appeared only at a concentration of $10 \mu\text{M}$ DSAQ where the molar ratio of the positive (porphyrin) to negative charges (DSAQ) is just 1; the effect of adding $10 \mu\text{M}$ DSAQ is equal to that of adding 0.3 M NaCl. The identical UV-VIS spectral pattern for Por-PPh in the presence of NaCl and the aromatic electrolyte (DSAQ) provides unambiguous evidence that the 'products' have the same structures. In other words, the spectra of the aggregates do not relate to a π - π stacked complex between the π -plane of the porphyrin and the π -plane of DSAQ. In our opinion, the neutralization hypothesis is inadequate for our system. In practice, Por-PPh as well as other cationic porphyrins also exist as aggregates in which the face-to-face geometry (H-aggregate) is dominant in the absence of electrolytes. This means that formation of H-aggregates does not need neutralization of the cationic charges. Addition of electrolytes causes a large red-shift, which suggests the formation of J-aggregates.^{10d,17} The aggregates have split Soret bands that return to the state before splitting upon large increases in the concentration of electrolytes. Therefore, we conclude that the morphology of the aggregates of Por-PPh, as induced by the addition of electrolytes, can be controlled precisely by the concentration of the electrolytes.

Table 6 Absorbance and wavelength of Por-PPh in DMSO

[Por-PPh]/ μM	$A(\lambda_{\text{max}}/\text{nm})$		$W_{1/2}/\text{nm}$		
0.1	0.034(421.6)	—	—	—	14.3
0.5	0.173(420.2)	—	—	—	14.3
1.0	0.348(420.7)	0.029(513.7)	0.023(551.7)	0.019(591.6)	0.019(645.8)
2.0	0.712(420.2)	0.043(514.1)	0.031(551.5)	0.024(591.0)	0.021(645.8)
5.0	1.786(420.0)	0.094(514.1)	0.057(550.4)	0.040(590.2)	0.033(645.7)
7.0	2.444(419.5)	0.133(515.1)	0.079(549.6)	0.052(591.1)	0.043(645.6)
10	2.526(419.0)	0.172(515.3)	0.100(551.4)	0.066(590.7)	0.052(645.6)

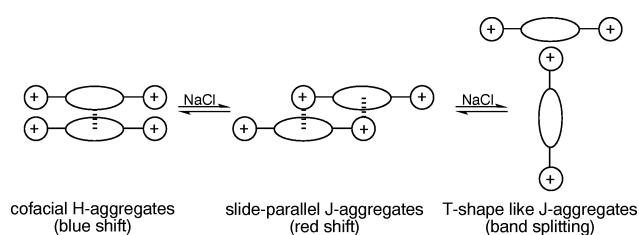
When the effect on aggregation of adding electrolytes was measured at 80 °C, spectral patterns were observed that were the same as those obtained at room temperature. This means that the transformation of the H-aggregate into the J-form is not affected by temperature. Different from the free base form, ZnPor–PPh (5 μM) was red-shifted by 24 nm in the presence of a definite amount of NaCl, but by only 10 nm in the presence of over 10 μM of DSAQ. From these shifted patterns, it can be said that the addition of NaCl to ZnPor–PPh solution induced the transformation^{10d,18} of H-aggregates into J-aggregates, whereas addition of DSAQ to the solution resulted in monomeric porphyrins with deaggregation of the H-form. It is probable that the zinc metal plays a role in strengthening the interaction between ZnPor–PPh and DSAQ.

In the H-aggregates of Por–PPh, ZnPor–PPh and Por–PBU, the π - π stacking is probably a loose interaction because of the bulky cationic sites so that the H-form transforms into the J-form when NaCl is added. What is the role of electrolytes in this transformation? If neutralization of the charges on the porphyrin causes the transformation, we should not need such high concentrations (molar range) of NaCl to neutralize the micromolar positive charges. Before considering these problems, it should be emphasized that the aromatic π -face has two negatively charged π -electron clouds that sandwich a positively charged σ -framework.^{5,19} This is the case for the porphyrin π -plane. Therefore, we propose the following mechanism for the transformation of aggregate geometry (Scheme 2).

Addition of a large amount of NaCl to water results in solvated Na⁺. Hence, the water-shelled Na⁺ attracts the π -surface of porphyrin by electrostatic interaction even over a long distance. This driving force weakens the van der Waals/hydrophobic interactions between the π -surfaces leading to deformation of the face-to-face geometry. As a response to the driving force from the Na⁺, the two π -surfaces in face-to-face dimer slide²⁰ to give an offset stacking¹⁹ where a new close contact caused by cation- π interactions between the peripheral phosphoniumyl charge and the π -plane of porphyrin can

be induced (discussed below). Mauzerall¹⁵ compared the effect of the size of cation on the electronic spectra of uroporphyrin III in aqueous solution and proposed that large cations, including quaternary ammoniums, pyridiniums and Cs⁺, are more likely to interact with uroporphyrin than are small cations, such as Li⁺, Na⁺ and K⁺. In our study, the ammoniumyl porphyrins did not exhibit J-aggregation spectral patterns in the presence of NaCl (data not listed).⁶ Considering the fact that the solvents having high polarizability prefer to interact with the highly polarizable porphyrin plane, the ability of phosphoniumyl porphyrins to form J-aggregates would be contributed to by the large atomic polarizability²¹ of phosphorus (24.5 Å³), which is larger than nitrogen (7.4 Å³). We think that the geometry of the aggregates of the phosphoniumyl porphyrins depends upon both the nature of the interaction and the structure of phosphonium. The van der Waals attractive force and/or hydrophobic interactions result in face-to-face geometry, but the electrostatic attractive force (cation- π interaction) gives offset J-geometry. On the basis of the extent of the red-shift, it can be said that the strength of the interactions between phosphonium and the π -surface of porphyrin would be larger for the -P⁺Ph₃ cation than for -P⁺Bu₃ cation; the polarizability of the phosphoniumyl residues is 40.20 and 33.63 Å³, respectively.¹² The transformation of H- into J-aggregates for Por–PPh that accompanies the addition of a small amount of DSAQ can also be ascribed to the fact that DSAQ weakens the van der Waals force between the π -surfaces of the dimeric porphyrins, which results in cation- π interactions between the peripheral -P⁺Ph₃ and the porphyrin plane. As a consequence, we suggest that the cation- π interactions between the large peripheral phosphonium cation and the large π -plane for phosphoniumyl porphyrins are promoted by the inorganic and aromatic salts.

In order to confirm the existence of the interactions between the phosphonium and the π -plane of porphyrins, we examined the effect of benzyltriphenylphosphonium chloride (BTTP), which has the same structural cationic residue as the triphenylphosphoniumyl porphyrins, on aggregates of Por–PPh and ZnPor–PPh. The Soret band was slightly red-shifted and the band-width narrowed as the concentration of BTTP increased (see Table 7). On the other hand, the absorption intensity returned to its initial level when the amount of BTTP was further increased. As a result, monomeric porphyrin formed completely in the presence of 100-fold BTTP; the spectral pattern was similar to that in DMSO solution, *i.e.*, cationic porphyrins in water aggregate only slightly as highly polarizable phosphonium salt is added. It became apparent that H-aggregates deaggregated on addition of BTTP to a solution of the above two porphyrins, and that the deaggregation procedure depended on the concentration of BTTP. This deaggregation can be explained by BTTP interacting strongly with the surface of the porphyrins. It can be concluded that



Scheme 2

Table 7 Effect of BTTP on the absorption spectra of Por–PPh and ZnPor–PPh^a

	[BTTP]/10 ⁻³ M	λ_{max} (nm)	$A(\lambda_{max}/nm)$	$W_{1/2}$ (Soret bands)			
Por–PPh	0	1.116(415.8)	0.064(517.6)	0.044(554.7)	0.027(585.5)	0.022(643.2)	28
	0.1	1.051(416.4)	0.070(519.7)	0.052(555.5)	0.034(587.6)	0.031(643.1)	28.8
	0.5	0.806(417.1)	0.076(520.7)	0.062(556.0)	0.046(591.4)	0.041(644.4)	27.5
	1.0	0.720(418.4)	0.077(520.5)	0.064(557.0)	0.049(591.9)	0.044(644.7)	28.8
	5.0	0.736(421.6)	0.071(519.9)	0.057(557.0)	0.044(590.0)	0.041(645.6)	20.5
	10	1.032(422.7)	0.067(518.8)	0.049(544.8)	0.034(590.8)	0.031(643.3)	16.8
ZnPor–PPh	0	1.699(420.7)		0.064(554.9)	0.029(595.5)		10.8
	0.1	1.740(420.7)		0.066(555.7)	0.029(595.5)		10.8
	0.5	1.726(421.1)		0.067(556.0)	0.030(594.6)		11.3
	1.0	1.618(420.9)		0.066(555.9)	0.031(596.3)		11.3
	5.0	1.596(422.7)		0.072(556.9)	0.034(596.5)		12.5
	10	1.432(424.2)		0.064(557.0)	0.031(596.8)		12.5

^a Concentration of the porphyrins was 5 μM.

the phosphonium chloride added prevents the cation- π aggregation of phosphoniumyl porphyrins, whereas NaCl induces a cation- π interaction between the peripheral phosphonium and the π -plane of phosphoniumyl porphyrins. By using ZnPor-DABCO, which is freely soluble in water, we investigated the interactions between ZnPor-DABCO and BTTP in aqueous solution using ^1H NMR. Fig. 4 shows the NMR spectra for BTTP, ZnPor-DABCO and a mixture of BTTP-(ZnPor-DABCO) (2 + 1). The peaks were identified by homodecoupling. All of the signals, including one benzyl and three phenyl groups for BTTP, were apparently shifted upfield (without free BTTP peaks) when ZnPor-DABCO was added to the BTTP solution. The most significant upfield shift (-1.6 ppm) is seen for the CH_2 peak with broadening. The order of upfield shift for the benzyl group is as follows: $\text{CH}_2 > o\text{-H} > m\text{-H} > p\text{-H}$. For the phenyl protons, the upfield order is also $o\text{-H}, m\text{-H} > p\text{-H}$. These upfield shifts must arise from the BTTP lying on the porphyrin plane where it is shielded by the strong π -current effect of porphyrin.²² This result provides unambiguous evidence that cationic BTTP strongly interacts with the π -surface of porphyrin to form a cationic- π complex.

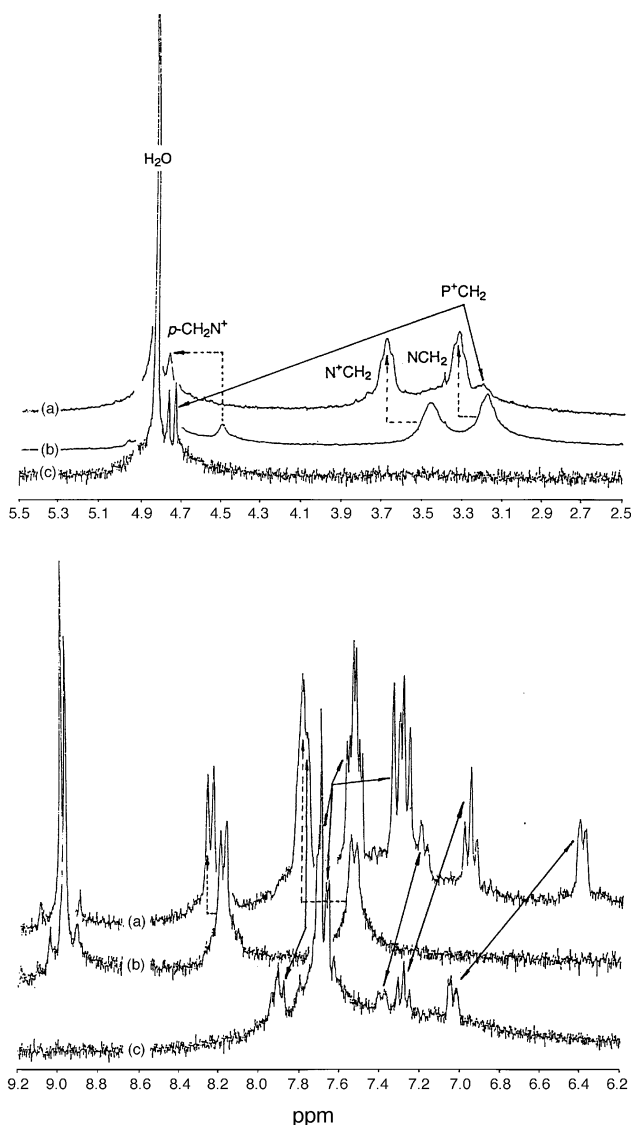


Fig. 4 ^1H NMR profiles of (a) BTTP (8×10^{-3} M), (b) ZnPor-DABCO (4×10^{-3} M) and (c) a mixture containing BTTP (8×10^{-3} M) and ZnPor-DABCO (4×10^{-3} M) in deuterated water. Upper: aliphatic proton region, 2.5–5.5 ppm. Bottom: aromatic proton region, 6.2–9.2 ppm. Temperature = 27 °C.

It can be seen from Fig. 4 that the protons on the periphery of the porphyrin, such as $p\text{-CH}_2$, CH_2CH_2 (on DABCO), $o\text{-H}$, $m\text{-H}$ (on the *meso*-phenyl ring) and the β -protons of ZnPor-DABCO, were shifted downfield; the downfield shifts for the β -protons and $o\text{-H}$, which are near the porphyrin plane, were very slight. Perhaps the interaction of BTTP with the π -surface of the porphyrin slightly increases the deshielding power of the porphyrin to the peripheral residues. We found that when the mixture of BTTP and ZnPor-DABCO was heated to 80 °C from 27 °C the upfield pattern for the protons of BTTP was not changed. This means, at least, that the interaction between the phosphonium and the porphyrin plane is very strong (a quantitative study of the interactions between the phosphoniums and porphyrins is in progress and will be published elsewhere).

We also performed a Job's plot for the mixture of BTTP and ZnPor-DABCO in aqueous solution (total concentration, 10 μM). Fig. 5 shows the results. Absorbances at different wavelengths, 421, 427 and 430 nm, were taken for this plot, each peak maximum, for the three wavelengths, appeared at nearly 0.5 molar composition, indicating that the porphyrin complexes with BTTP at a ratio of 1 : 1.

We know from the above discussion that the behavior of Por-PBu in NaCl is similar to that of Por-PPh, but the response of Por-PBu to DSAQ apparently differed to that of Por-PPh. No split of the Soret band appeared on adding DSAQ to this porphyrin. Job's plots for Por-PPh and Por-PBu with DSAQ were also examined. As shown in Fig. 6, the Job's plot for the (Por-PBu)-DSAQ mixture showed a maximum for X_p (mol fraction of porphyrin) of 0.67 at 414 nm and of 0.5 at 422 nm, indicating that the complexes between Por-PBu and DSAQ existed not only in the ratio of 2 : 1 (Por : DSAQ), but also 1 : 1. For the (Por-PPh)-DSAQ mixture, however, no information about the stoichiometry between Por-PPh and DSAQ was observed.

For the typical cationic porphyrins, such as tetrakis(methylpyridiniumyl)porphyrin and tetrakis(trimethylammoniumphenyl)porphyrin, the cationic centre is located at a fixed position. Compared with this, the cationic sites on our cationic porphyrins are quite 'fruitful' as the cationic atoms freely rotate in relation to the methylene carbon. This rotational feature must be important in the construction of the geometry of the J-aggregates. We propose that the splitting of the Soret band might be related to T-shape-like geometry (Scheme 2). As reported by Maruyama and co-workers in their covalently linked porphyrin dimer or polymer system, the Soret band split appears as the two π -surfaces adopt a geometry having a dihedral angle.²³ That non-covalent porphyrin aggregates

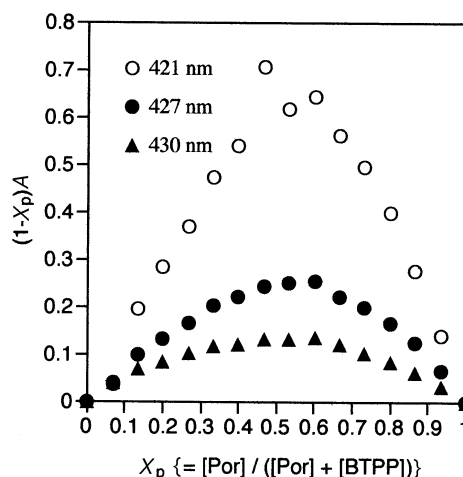


Fig. 5 Job's plot for (ZnPor-DABCO)-BTTP in H_2O at different wavelengths. Total concentration = 1×10^{-5} M.

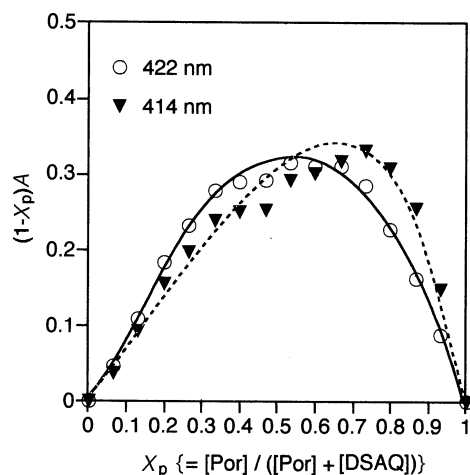


Fig. 6 Job's plot for (Por-PBu)-DSAQ in H_2O at different wavelengths. Total concentration = 1×10^{-5} M.

result in such apparent Soret band splits indicates that the aggregates have a highly specific geometry with a stable dihedral angle supported by a strong attractive force.

Conclusions

Water soluble cationic porphyrins bearing phosphonium residues have a very strong self-aggregation power exhibiting π - π stacking geometry in pure water and in low polarizability solvents. This aggregation depends upon the concentration of the porphyrins. In particular, face-to-face aggregation takes place below concentrations of $1 \mu\text{M}$. Addition of NaCl or organic salt (DSAQ) to aqueous solutions of the porphyrins can induce transformation of the geometry from H- (face-to-face) to J-aggregates. However, the formation and structure of the J-aggregates are very sensitive to the structure of cationic residues. In the cationic porphyrin systems used here the flat π -surface of the porphyrin is not altered structurally by the peripheral cationic sites because the cationic centre is linked to the *meso*-phenyl ring by a methylene bridge. Therefore, we conclude that self-aggregation of the cationic porphyrins in water is determined by the structure of the cationic site, and that the cation- π interaction between the peripheral cations and the porphyrin plane also plays an important role in the self-aggregation. Our work provides an important example in investigating the relations between the self-assembly properties of cationic porphyrins and the peripheral cationic structures. We believe that the concept of cation- π interaction between the porphyrin face and the phosphoniumyl cation has high potential utility in the building up of supramolecular systems in aqueous solution. Further related work is in progress.

Experimental

General

^1H NMR (250 MHz) spectra were recorded on a Bruker AC 250P spectrometer relative to an internal standard of TMS in deuterated organic solvent or an internal standard of H_2O (4.83 ppm) in deuterated water. Stock solutions of cationic porphyrins were prepared as 1×10^{-3} M and used in dilution. Absorption spectra were recorded in 1.0 cm pathlength quartz cells at room temperature on a Hitachi 150-20 spectrophotometer using the solvents as references.

Reagents and solvents

Triphenylphosphine, tri-*n*-butylphosphine, pyrrole and DABCO were purchased from Tokyo Kasei Co. and used

without further purification. Chloranil, boron trifluoride-diethyl ether, triethylamine, NaCl and DSAQ were purchased from Wako Pure Chemical Co. and used without further purification. DMF was used as the reaction solvent after drying over 4 \AA molecular sieve. The solvents (DMSO, MeOH, DMF, acetonitrile, acetone and chloroform) used in the UV-VIS analysis were a special grade of Wako Pure Chemical Co. Deionized water was used after distillation. BTTP was synthesized by reaction of triphenylphosphine and benzyl chloride, and the product was recrystallised three times from ether. TTP was obtained from Aldrich and purified by column chromatography using chloroform as eluent. *p*-Chloromethylbenzaldehyde, CMPP and the cationic porphyrins were synthesized according to a previously reported method.⁶

CMPP. To a three-neck round bottomed flask equipped with a condenser, a three-way stop-cock and a gas-bubbling tube, *p*-chloromethylbenzaldehyde (0.31 g, 2.0 mmol), pyrrole (0.14 g, 2.0 mmol) and chloroform (200 ml, dried over 4 \AA molecular sieves) were added. The mixture was stirred with bubbling by Ar for 10 min and boron trifluoride-diethyl ether (0.01 ml, 0.025 mmol) was added. Then the mixture was stirred at room temperature for 1 h. Then, triethylamine (0.113 ml, 1.51 mmol) and chloranil (0.37 g, 1.50 mmol) were added and the mixture was refluxed for 1 h. The solvent was then removed under reduced pressure. The residue was dissolved in dichloromethane and any non-soluble impurities filtered off. The filtrate was concentrated to 30 ml, and 45 ml of methanol was added. This solution was concentrated until the total volume was reduced to 10 ml. The mixture was then filtered and the filtrate evaporated off. The solid residue was passed through a silica column using chloroform as eluent. Yield, 0.19 g (47.5%). ^1H NMR (250 MHz, in CDCl_3 , TMS as internal standard) δ -2.8 (s, 2 H), 5.0 (s, 8 H), 7.7-7.8 (d, 8 H), 8.1-8.2 (d, 8 H), 8.8 (s, 8 H). UV-VIS (in CHCl_3) $\lambda_{\text{max}}/\text{nm}$ 418.9, 515.4, 541.7, 590.0, and 648.4. SIMS (m/z) 808.

ZnCMPP. This was obtained according to a standard method by reaction of free base CMPP with $\text{Zn}(\text{OAc})_2$ in $\text{MeOH}-\text{CHCl}_3$ solution. The yield isolated by silica column chromatography (CHCl_3 as eluent) was 85%. ^1H NMR (250 MHz, in CDCl_3 , TMS as internal standard) δ 5.0 (s, 8 H), 7.6-7.8 (d, 8 H), 8.1-8.3 (d, 8 H), 8.9 (s, 8 H). UV-VIS (in CHCl_3) $\lambda_{\text{max}}/\text{nm}$ 423.0, 548.6 and 594.6. SIMS (m/z) 870.

Cationic porphyrins. The tetra-cationic porphyrins were prepared according to the previous method⁶ from the reactions of CMPP (or ZnCMPP) with excess (10 equiv. per ClCH_2 group) of the corresponding phosphines (or amines) in DMF at 80°C for 2 d (but 2 h for DABCO) under argon. Within this reaction time, the ClCH_2 groups completely reacted with the phosphines (or amines) as confirmed by ^1H NMR. The DMF was then removed under reduced pressure and the residues dissolved in a small amount of methanol. This mixture was then poured into ether to precipitate the cationic porphyrin. The solid obtained was reprecipitated twice in the same manner. The method yielded quantitative amounts of the cationic porphyrins.

Por-PBu. ^1H NMR (250 MHz, in $[\text{D}_6]\text{DMSO}$, TMS as internal standard) δ -2.9 (s, 2 H), 0.9-1.1 (t, 36 H), 1.5-1.6 (m, 48 H), 2.5 (m, 24 H), 4.2-4.3 (d, 8 H), 7.8-7.9 (d, 8 H), 8.2-8.3 (d, 8 H), 8.8 (s, 8 H). UV-VIS (in MeOH) $\lambda_{\text{max}}/\text{nm}$ 414.8, 512.0, 550.7, 592.3 and 644.0. FABMS (m/z) 1545, 1546 ($\text{M}^{4+} + 2\text{Cl}^- - \text{H}^+$)⁺, 1508, 1509, 1510, 1511 ($\text{M}^{4+} + \text{Cl}^- - \text{H}^+$)⁺, 1270.8, 1271.8 ($\text{M}^{4+} - \text{PBu}_3^+ - 2\text{H}^+$)⁺, 1069.6, 1070.6 ($\text{M}^{4+} - 2\text{PBu}_3^+ - \text{H}^+$)⁺, 868.5, 869.5 ($\text{M}^{4+} - 3\text{PBu}_3^+$)⁺, 1472, 1473 ($\text{M}^{4+} - 2\text{H}^+$)²⁺, 736.5

$[(M^{4+} - 2H^+)^{2+}/2]$, 636.0 $[(M^{4+} - PBu_3^+ - H^+)^{2+}/2]$; calc. 1476.1 for M^{4+} ($C_{96}H_{142}N_4P_4$).

Por-PPh. 1H NMR (250 MHz, in $[^2H_6]DMSO$, TMS as internal standard) δ -3.1 (s, 2 H), 5.6–5.7 (d, 8 H), 7.3–8.0 (m, 76 H), 8.76 (s, 8, H). UV–VIS (in MeOH) λ_{max}/nm 414.8, 519.2, 555.6, 585.2 and 642.8. FABMS (m/z) 1711.8, 1712.8 ($M^{4+} - 3H^+$) $^+$, 1449.6, 1450.6 ($M^{4+} - PPh_3^+ - 2H^+$) $^+$, 1188.7, 1189.6 ($M^{4+} - 2PPh_3^+ - H^+$) $^+$, 927.4, 928.4 ($M^{4+} - 3PPh_3^+$) $^+$, 1713, 1714 ($M^{4+} - 2H^+$) $^{2+}$, 856.5, 857.0 $[(M^{4+} - 2H^+)^{2+}/2]$; calc. 1716.7 for M^{4+} ($C_{120}H_{96}N_4P_4$).

ZnPor-PPh. 1H NMR (250 MHz, in $[^2H_4]$ methanol, TMS as internal standard) δ 5.2–5.3 (d, 8 H), 7.3–7.4 (d, 8 H), 7.6–8.0 (m, 68 H), 8.7 (s, 8 H). UV–VIS (in MeOH) λ_{max}/nm 423.5, 557.3 and 596.7; (in $CHCl_3$) 426.9, 558.2 and 603.5.

ZnPor-PBu. 1H NMR (250 MHz, in $[^2H_4]$ methanol, TMS as internal standard) δ 1.1–1.3 (t, 36 H), 1.5–1.7 (m, 48 H), 2.4–2.5 (m, 24 H), 4.0–4.1 (d, 8 H), 7.7–7.8 (d, 8 H), 8.2–8.3 (d, 8 H), 8.7 (s, 8 H). UV–VIS (in MeOH) λ_{max}/nm 422.5, 557.0 and 596.0

ZnPor-DABCO. 1H NMR (250 MHz, in $[^2H_6]DMSO$, TMS as internal standard) δ 3.2–3.4 (t, 24 H), 3.5–3.7 (t, 24 H), 4.9 (s, 8 H), 7.9–8.0 (d, 8 H), 8.3–8.4 (d, 8 H), 8.9 (s, 8 H). UV–VIS (in MeOH) λ_{max}/nm 421.0, 555.3 and 595.4

We give great thanks to N. Morisaki (University of Tokyo) for the FABMS measurement. We also appreciate the practical assistance of K. Tanabe and K. Kaigake for the NMR and SIMS measurements.

References

- 1 A. Warshel and W. W. Parson, *J. Am. Chem. Soc.*, 1987, **109**, 6152; J. T. Groves and T. P. Farrell, *J. Am. Chem. Soc.*, 1989, **111**, 4998; K. Kalyanasundaram, *J. Chem. Soc., Faraday Trans.*, 2, 1983, **79**, 1365; B. Armitage, P. A. Klekotka, E. Obilinger and D. F. O'Brien, *J. Am. Chem. Soc.*, 1993, **115**, 7920.
- 2 (a) F. J. Vergeldt, R. B. M. Koehorst, A. van Hoek and T. J. Schaafsma, *J. Phys. Chem.*, 1995, **99**, 4397 and references cited therein; (b) K. Kano, M. Takei and S. Hashimoto, *J. Phys. Chem.*, 1990, **94**, 2181; (c) K. Kalyanasundaram, *Inorg. Chem.*, 1984, **23**, 2453; (d) K. Kano, T. Nakajima, M. Takei and S. Hashimoto, *Bull. Chem. Soc. Jpn.*, 1987, **60**, 1281; (e) R. F. Pasternack, P. Huber, P. Boyd, G. Engasser, L. Francesconi, E. Gibbs, P. Fasella, G. C. Venturo and L. deC. Hinds, *J. Am. Chem. Soc.*, 1972, **94**, 4511; (f) R. L. Brookfield, H. Ellul and A. Harriman, *J. Photochem.*, 1985, **31**, 97.
- 3 M. R. Waisielewski, *Chem. Rev.*, 1992, **92**, 435.
- 4 (a) G. Markl, M. Reiss, P. Kreitmeier and H. Noth, *Angew. Chem., Int. Ed. Engl.*, 1995, **34**, 2230; (b) S. Arimori, M. Takeuchi and S. Shinkai, *Chem. Lett.*, 1996, **77**; (c) T. Mizutani, H.

Koyama, T. Ema, A. Nomura, T. Yoshita and H. Ogoshi, *Chem. Lett.*, 1995, 941; (d) H. J. Schneider and M. Wang, *J. Org. Chem.*, 1994, **59**, 7473.

- 5 D. A. Dougherty, *Science*, 1996, **271**, 163.
- 6 R-H. Jin, S. Aoki and K. Shima, *Chem. Commun.*, 1996, 1939.
- 7 (a) K. Kano, T. Nakajima and S. Hashimoto, *J. Phys. Chem.*, 1987, **91**, 6614; (b) N. C. Maiti, M. Ravikanth, S. Mazumdar and N. Periasamy, *J. Phys. Chem.*, 1995, **99**, 17192.
- 8 (a) K. Kano, T. Sato, S. Yamada and T. Ogawa, *J. Phys. Chem.*, 1983, **87**, 566; (b) J. A. Shelnutz, *Inorg. Chem.*, 1983, **22**, 2535; (c) K. Kano, M. Takei and S. Hashimoto, *J. Phys. Chem.*, 1990, **94**, 2181.
- 9 D. L. Akins, H-R. Zhu and C. Guo, *J. Phys. Chem.*, 1996, **100**, 5420; K. M. Kadish, B. G. Maiya and C. Araullo-McAdams, *J. Phys. Chem.*, 1991, **95**, 427; K. Kemnitz and T. Sakaguchi, *Chem. Phys. Lett.*, 1992, **196**, 497.
- 10 (a) E. S. Enerson, M. A. Conlin, A. E. Rosenoff, K. S. Norland, H. Rodriguez, D. Chin and G. R. Bird, *J. Phys. Chem.*, 1967, **71**, 2396; (b) L. L. Shipman, J. R. Norris and J. J. Katz, *J. Phys. Chem.*, 1976, **80**, 877; (c) W. W. Parson and A. Warshel, *J. Am. Chem. Soc.*, 1987, **109**, 6152; (d) O. Q. Munro and H. M. Marques, *Inorg. Chem.*, 1996, **35**, 3768.
- 11 T. Shimidzu and T. Iyoda, *Chem. Lett.*, 1981, 853; V. Thanabal and V. Krishnan, *J. Am. Chem. Soc.*, 1982, **104**, 3643; A. C. Bookser and T. C. Bruice, *J. Am. Chem. Soc.*, 1991, **113**, 4208.
- 12 The molecular polarizabilities are cited from the literature and are calculated according to the equation $\alpha/\text{\AA}^3 = (4/N)[\sum_A \tau_A]^2$, where N is the number of electrons in the molecules and τ_A are the atomic components for atoms in particular hybrid configurations. See K. J. Miller and A. Savchik, *J. Am. Chem. Soc.*, 1979, **101**, 7206.
- 13 K. Kano, T. Hayakawa and S. Hashimoto, *Bull. Chem. Soc. Jpn.*, 1991, **64**, 778.
- 14 D. B. Smithrud and F. Diederich, *J. Am. Chem. Soc.*, 1990, **112**, 339.
- 15 D. Mauzerall, *Biochemistry*, 1965, **4**, 1801.
- 16 R. Karaman and T. C. Bruice, *J. Org. Chem.*, 1991, **56**, 3470.
- 17 K. Kano, T. Nakajima and S. Hashimoto, *J. Phys. Chem.*, 1987, **91**, 6614; N. C. Maiti, M. Ravikanth, S. Mazumdar and N. Periasamy, *J. Phys. Chem.*, 1995, **99**, 17192.
- 18 D. C. Barber, R. A. Freitag-Beeston and D. G. Whitten, *J. Phys. Chem.*, 1991, **95**, 4074.
- 19 C. A. Hunter and J. K. M. Sanders, *J. Am. Chem. Soc.*, 1990, **112**, 5525.
- 20 C. A. Hunter, *Chem. Soc. Rev.*, 1994, 101.
- 21 X-M. Zhang and F. G. Bordwell, *J. Am. Chem. Soc.*, 1994, **116**, 968.
- 22 C. B. Storm and A. H. Corwin, *J. Org. Chem.*, 1964, **29**, 3700.
- 23 A. Osuka and K. Maruyama, *J. Am. Chem. Soc.*, 1988, **110**, 4454; T. Nagata, A. Osuka and K. Maruyama, *J. Am. Chem. Soc.*, 1990, **112**, 3054; K. Susumu, H. Segawa and T. Shimidzu, *Chem. Lett.*, 1995, 929.

Paper 7/03965D; Received 6th June, 1997